

# Field-Plate Geometry Dependent Electrostatics and Strain Mapping in AlGaAs/GaAs HEMTs



R. K. Nanda, T. P. Dash

**Abstract:** GaAs based power transistors provides higher switching speed compared to conventional Si transistors. The high electron mobility transistors (HEMTs) with AlGaAs/GaAs have got recent attentions for alternative suitable candidate for high frequency operation. The primary focus of the work is to study the electrostatics and stress/strain profile mapping due to the presence of field plate in AlGaAs/GaAs high electron mobility transistors. Using TCAD simulations, we examine the stress strain profile mapping as a function of field plate geometry and also study the electrostatics as function of field plate geometry and applied electric field.

**Index Terms:** HEMT, AlGaAs/GaAs, field plate, TCAD, Electric field, Stress/Strain mapping.

## I. INTRODUCTION

In the quest for alternative solutions for Si CMOS, III-V MOSFETs are being proposed. Due to their outstanding transport properties, III-V semiconductors hold a promise of reduced CMOS supply voltage without compromising the performance. Semiconductors composed of materials from columns III and V of the periodic table are promising candidates for use as channel in MOS transistors (for both the types of carriers). Due to their outstanding electronic properties, III-V materials such as GaAs, InAs and In<sub>1-x</sub>Ga<sub>x</sub>As alloys have been widely used in the fields of optical communication, instrumentation and detection. The basic building block now in III-V technology for high frequencies is the High Electron Mobility Transistors (HEMT). Nevertheless, the HEMTs have also their limits in terms of the scaling laws, such as gate length and thickness of the heterostructures. Multiple field plates (FP) may be used to achieve both high breakdown voltage and high frequency operation.

Today, the III-V MOSFET technology is a very active area of research and has recently been included in the ITRS roadmap (International Technology Roadmap for Semiconductors). To benefit from the excellent intrinsic performance of III-V materials, several critical issues need to be resolved [1].

AlGaAs/GaAs possesses “wurtzite” crystal structure (hexagonal crystal system) and wide bandgap energy of 3.4 eV. It becomes an extremely preferable candidate in high voltage switching operations and power electronics circuits due to its wide bandgap, high electron mobility and high break down voltage [2]. The implementation of field plate (FP) in GaN based HEMTs is very well known technique to improve the performances [3]. The role of a FP is to modify the electric field profile and to decrease its peak value on the drain side of the gate edge, hence reducing high-field trapping effects and increasing breakdown voltage. Multiple field plates may be used to achieve both high breakdown voltage and high frequency operation. Due to the piezoelectric nature of GaN, the 2DEG in AlGaN/GaN HEMT could be engineered by strain [4-5]. It has been reported that the gate breakdown occurs at the drain-side edge of that gate electrode due to the high electric field peak, via avalanche breakdown and thermally assisted tunneling [6].

At the edge of the gate, the electric field intensity can be decreased by the introduction of field plate which also diminishes the probability of electron trapping [7]. Understanding material and process limits for high breakdown voltage AlGaN/GaN HEMTs have been reported [8]. Due to the piezoelectric nature of AlGaAs/GaAs, the 2D electron gas (2DEG) in AlGaAs/GaAs HEMT can also be engineered by strain. Because the modulation of strain becomes more pronounced with device scaling, the influence of the variation in strain on the device characteristics is of great concern. Mechanical stress is an important factor influencing the performance of GaAs-based devices. Material/electronic properties of compound semiconductors are dependent on stress. In highly piezoelectric materials like AlGaAs/GaAs, mechanical stress directly influences the piezoelectric polarization, and hence the charge density of the 2-D electron gas [9]. Since stress is a major factor in the operation and performance in AlGaAs/GaAs HEMT devices, a thorough understanding of the impact of stress on performance can lead to improvements in device design.

Manuscript published on November 30, 2019.

\* Correspondence Author

**R. K. Nanda\***, Department of EICE, Siksha O Anusandhan (Deemed to be University), Bhubaneswar, India

**T. P. Dash**, Department of EICE, Siksha O Anusandhan (Deemed to be University), Bhubaneswar, India.

© The Authors. Published by Blue Eyes Intelligence Engineering and Sciences Publication (BEIESP). This is an [open access](https://creativecommons.org/licenses/by-nc-nd/4.0/) article under the CC-BY-NC-ND license <http://creativecommons.org/licenses/by-nc-nd/4.0/>.

In this work, we perform simulations of a planar AlGaAs/GaAs HEMTs to investigate the effects stress strain and their mapping using TCAD simulation tool.

Finite element modelling (FEM) of the mechanical stress in HEMT devices was done using VictoryDevice [10]. In this paper, we have the five Sections including the introduction part as Section I. The design aspects of field plate based AlGaAs/GaAs HEMTs are presented in Section II. The device structure detail and stress simulation basics and field plate geometry dependent stress profiles are presented. Section III includes the device structure detail and simulation environment. The results and discussion of the stress/strain profiles are presented in Section IV. Conclusions drawn from this study are presented in Section V.

II. MECHANICAL STRAIN/STRESS MODELLING

Mechanical stress represents a force per unit area. It is expressed in Pa or N/m<sup>2</sup>. By convention, tensile stress is represented as positive while a compressive stress as negative. To represent the general state of stress at a given point of a material, one uses the tensorial formalism. Under the effect of a mechanical stress, a material is deformed. This deformation is not just in the direction of the stress. In addition the deformation depends on the mechanical properties of the material. It is assumed that the stress state of the material considered is in the elastic domain, i.e. the stresses are sufficiently low not to generate plastic deformations, irreversible. This requires that the strain will be less than the yield strength of the material. In addition we will assume that the deformations are proportional to the strain, i.e., the quantitative determination of the state of deformation of the material can be obtained using the formalism of linear elasticity theory.

Hooke’s law relates the stress and strain with the following expression

$$\vec{\sigma} = C \cdot \vec{\epsilon} \tag{1}$$

where  $\vec{\sigma}$ , denotes stress tensor and  $\vec{\epsilon}$  denotes strain tensors and C denotes elastic coefficient tensor. For a hexagonal crystal system  $\vec{\sigma}$ ,  $\vec{\epsilon}$ , and C can be expressed Following Voigt notation<sup>17</sup> as follows:

$$\vec{\sigma} = \begin{bmatrix} \sigma_{xx} \\ \sigma_{yy} \\ \sigma_{zz} \\ \sigma_{yz} \\ \sigma_{zx} \\ \sigma_{xy} \end{bmatrix} \quad \vec{\epsilon} = \begin{bmatrix} \epsilon_{xx} \\ \epsilon_{yy} \\ \epsilon_{zz} \\ 2\epsilon_{yz} \\ 2\epsilon_{zx} \\ 2\epsilon_{xy} \end{bmatrix} \quad C = \begin{bmatrix} C_{11} & C_{12} & C_{13} & 0 & 0 & 0 \\ C_{12} & C_{11} & C_{13} & 0 & 0 & 0 \\ C_{13} & C_{13} & C_{33} & 0 & 0 & 0 \\ 0 & 0 & 0 & C_{44} & 0 & 0 \\ 0 & 0 & 0 & 0 & C_{44} & 0 \\ 0 & 0 & 0 & 0 & 0 & \frac{C_{11}-C_{12}}{2} \end{bmatrix} \tag{2}$$

For a film if the growth direction in Z axis, then the stress will take place in two perpendicular directions and it will in a biaxial stress state. The strain tensor components are different

along different directions. They can be expressed in terms of their ‘lattice constants’ as:

$$\epsilon_{xx} = \epsilon_{yy} = \frac{a-a_0}{a_0}; \quad \epsilon_{zz} = \frac{c-c_0}{c_0} \tag{3}$$

where  $a_0$ ,  $c_0$  and a, c are epilayer’s unit cell parameters for relaxed and strained epilayer’s respectively.

$$\sigma = \left( c_{11} + c_{12} - \frac{2c_{13}^2}{c_{33}} \right) \epsilon \tag{4}$$

where  $\sigma = \sigma_{xx} = \sigma_{yy}$ , and  $\forall i \neq j, \sigma_{ij} = 0$

$$\text{and } \epsilon_{zz} = -\frac{2c_{13}}{c_{33}} \epsilon \tag{5}$$

where  $\epsilon = \epsilon_{xx} = \epsilon_{yy}$

Therefore, for the biaxial stress condition, the stress-strain relation is given by equation 4 and equation 5 correlates the deformation  $\epsilon_{zz}$  (along direction Z-axis) for any lateral deformation  $\epsilon$ . In uniaxial stress condition,  $\sigma_{xx} \neq \sigma_{yy} = \sigma_{zz} = 0$ , the correlation between  $\epsilon_{xx}$  and  $\epsilon_{zz}$  can be expressed from equations 1 and 2 as:

$$\epsilon_{zz} = -\frac{c_{13}(c_{11}-c_{12})}{c_{11}c_{33}-c_{13}^2} \epsilon_{xx} \tag{6}$$

For heteroepitaxial films, from equations 5 and 6, we can express the deformed lattice parameter along the growth direction as:

$$c = c_0 \left[ 1 - \frac{2c_{13}}{c_{33}} \left( \frac{a-a_0}{a_0} \right) \right] \tag{7}$$

for biaxial stress condition and

$$c = c_0 \left[ 1 - \left\{ \frac{c_{13}(c_{11}-c_{12})}{c_{11}c_{33}-c_{13}^2} \right\} \left( \frac{a-a_0}{a_0} \right) \right] \tag{8}$$

for uniaxial stress condition.

From Young’s modulus (E) and Poisson’s ratio ( $\nu$ ), the stiffness (tensor) of the material can be calculated as follows:

$$\begin{aligned} C_{1111} &= C_{2222} = C_{3333} = E(1-\nu)/(1+\nu)(1-2\nu) \\ C_{1122} &= C_{2233} = C_{1133} = E\nu/(1+\nu)(1-2\nu) \\ C_{2211} &= C_{3322} = C_{3311} = E\nu/(1+\nu)(1-2\nu) \\ C_{1212} &= C_{3131} = C_{2323} = E/2(1+\nu) \end{aligned}$$

To calculate the stress, we incorporated "stress evolution" or "stress history" model. Material properties of various materials used in stress simulation are presented in Table-1



Material	Young's modulus (Dyne/cm <sup>2</sup> )	Poisson ratio	Thermal expansion (W.cm <sup>-1</sup> .K <sup>-1</sup> )
AlGaAs	2.60e+12	3.00e-01	1.44e-05
GaAs	8.59e+11	3.10e-01	5.73e-06
Sapphire	3.45e+12	3.50e-01	8.40e-06
SiO <sub>2</sub>	2.00e+11	2.00e-01	1.206e-07
Isotropic Aluminum	7.00e+11	3.50e-01	-

### III. DEVICE STRUCTURE

Fig. 1 shows the schematic cross-section view of the AlGaAs/GaAs HEMT with multiple field plates. A nominal composition (x) of 0.3 was assumed in simulations. Linear elasticity was assumed to be valid for all the stress conditions considered. In this work, a 2D AlGaAs/GaAs HEMT structure with the stress distribution resulting from intrinsic stress was generated.

The stress induced underneath the gate region depending on the gate length has been investigated. The stress distributions and profiles were simulated using Silvaco VictoryStress [11].

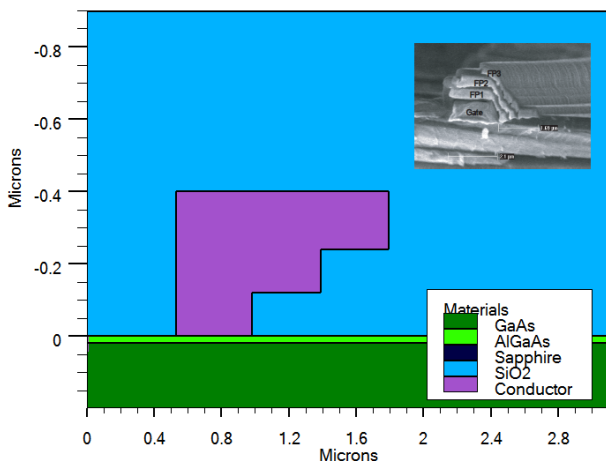


Fig. 1: Schematic of the device structure used in simulation. In inset, experimental structure of a typical multi field plate device is shown. VictoryStress tool is used to compute the stress distribution in the structure for various materials used in the device.

### IV. RESULTS AND DISCUSSIONS

#### A. Stress Analysis

A common technique to combine complex stresses is to calculate the von Mises equivalent stress in the structure. The mechanical stress distribution was computed using the linear elasticity theory discussed before and the material parameters presented in Table-1. The von Mises stress is traditionally used to examine plastic yielding, where the critical value being compared to represents the onset of plastic yielding. For the purposes of this study, the von Mises stress will be used to understand the uniaxial stresses occurring in the device. Materials intrinsic stress due to the presence of the field plate is examined. Stress generated are found to be compressive in nature. Fig. 2 shows the Von Mises stress around the field plate at an applied drain voltage of 100V. The stress is found to be in the range of  $4.4 \times 10^8$  to  $6.5 \times 10^8$

dynes/cm. The stress in the XX-direction is shown in Fig. 3. Biaxial stress in AlGaAs/GaAs compressive stress field induces compressive stress near the gate. The biaxial-tensile stress is observed in the AlGaAs/GaAs near the gate foot, whereas it becomes compressive near the ohmic contact region. Simulated stress distributions in the devices. In the device with 0.1  $\mu\text{m}$  gate length, more intensive compression is developed at the gate edge. There are more compressive stresses in the AlGaAs/GaAs region underneath the gate.

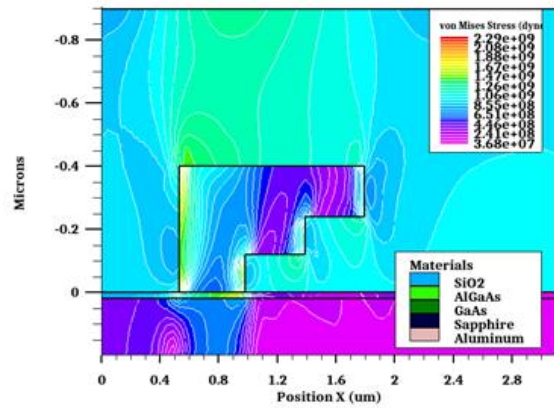


Fig. 2: The Von Mises stress distribution in the field plate region of the AlGaAs/GaAs HEMT structure.

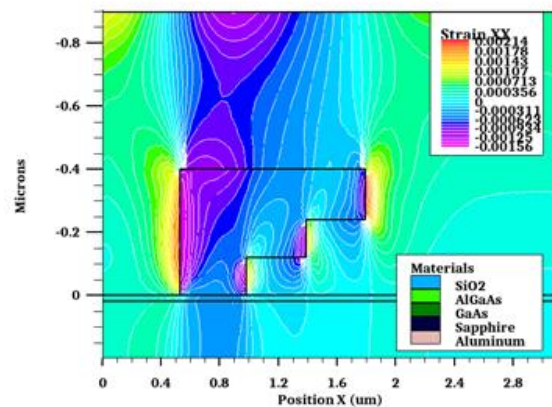


Fig. 3: XX-stress distribution in the field plate region of the AlGaAs/GaAs HEMT structure.

#### B. Electrostatics in AlGaAs/GaAs HEMTs

The electric field distribution (at an applied drain voltage of 100V) due to the presence of multiple field plate is shown in Fig. 4. It is observed that the peak field distribution occurs at the edge of the field plate. The potential distribution beneath the field plate is shown in Fig. 4. The role of a FP is to change the electric field profile and to drop its peak value on the drain side of the gate edge, which is clearly visible from Fig. 4. Biaxial stress map shows both the tensile and compressive stress regions surrounding the field plate.

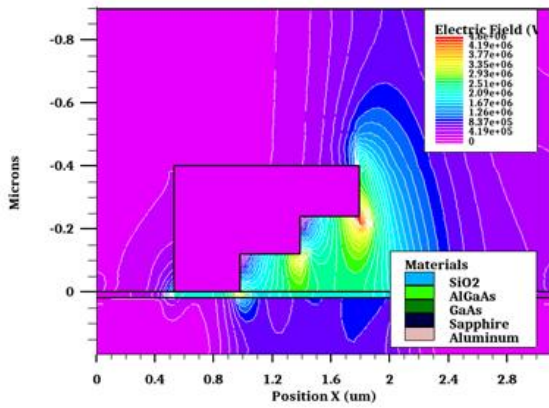


Fig. 4.: Electric field distribution in the field plate region of the AlGaAs/GaAs HEMT structure. The peak field distribution occurs at the edge of the field plate.

Other electrical parameters of AlGaAs/GaAs HEMTs such as, the conduction band, valence band, electron mobility and potential at an applied drain voltage of 100V are shown in Figs. 5 through 8. A generic conclusion can be drawn that the geometry of field plate has a tremendous effect on the parameter profile in the device. Fig. 9 shows the electric field distribution at field plate edge as a function of drain voltage (a) 20V, (b) 50V, (c) 80V and (d) 100V, respectively.

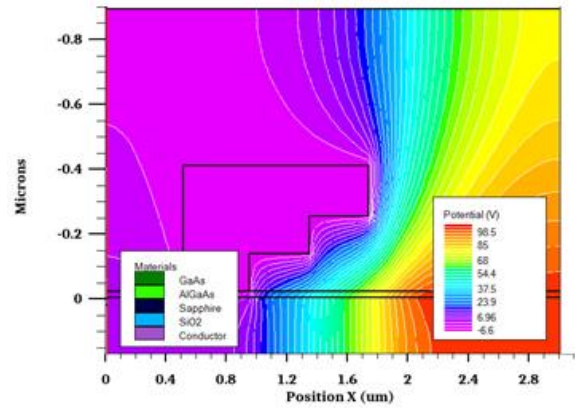


Fig. 7.: Potential distribution at the field plate edge of the AlGaAs/GaAs HEMT structure.

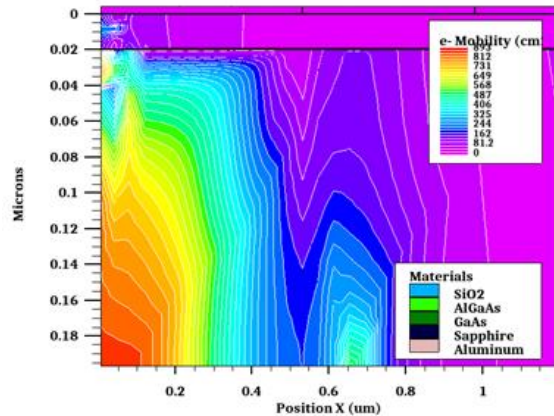


Fig. 8: Electron mobility distribution in the field plate region of the AlGaAs/GaAs HEMT structure.

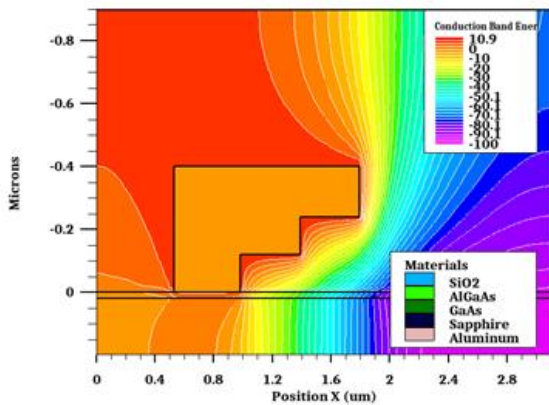


Fig. 5: Conduction band profile in the field plate region of the AlGaAs/GaAs HEMT structure.

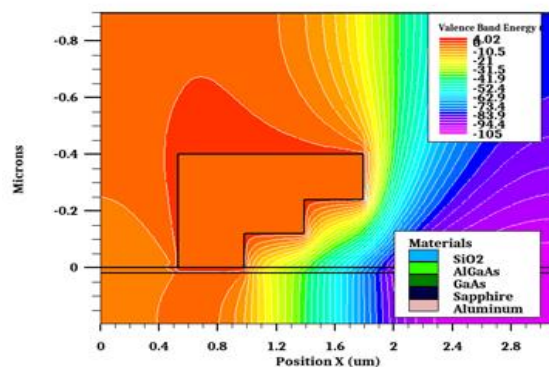


Fig. 6: Valence band profile in the field plate region of the AlGaAs/GaAs HEMT structure.

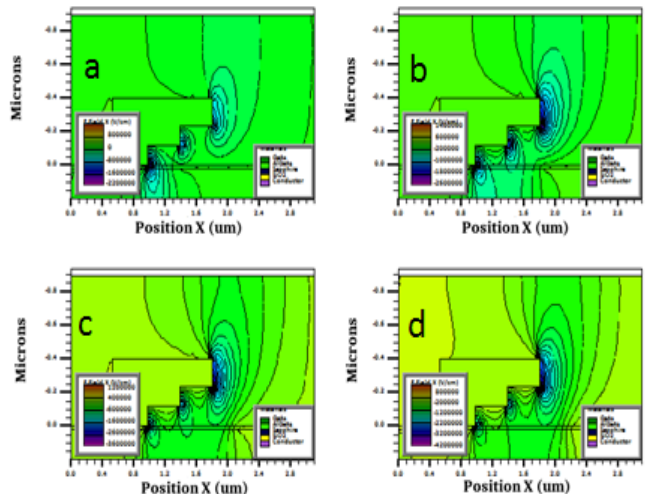


Fig. 9: Electric field distribution at field plate edge as a function of drain voltage (a) 20V, (b) 50V, (c) 80V and (d) 100V, respectively.

## V. CONCLUSION

Using TCAD simulations, we have shown that the mechanical stress are present in extremely localized regions such as the field plate/gate corner of AlGaAs/GaAs HEMTs. The design methodology presented in this work has a great potential of high voltage AlGaAs/GaAs HEMT design for power switching applications. The field plate geometry is found to significantly change the stress profiles. The field plate length, the insulator thickness and AlGaAs/GaAs layer doping concentration are the design parameters for the stress/strain simulations. ~~It can be~~ observed that the strain can induce significant amount of piezoelectric charges in the submicron gate region. Therefore, strain engineering is shown to be an effective approach to study the design issues of AlGaAs/GaAs HEMTs.

## REFERENCES

1. International Technology Roadmap for Semiconductors (ITRS). 2015 edition. Online: <http://www.itrs.net> (visited on May 21, 2019).
2. U. K. Mishra, P. Parikh, and Y.-F. Wu, "AlGaIn/GaN HEMTs— An overview of device operation and applications," Proc. IEEE, vol. 90, pp. 1022–1031, 2002.
3. S. Karmalkar and U. K. Mishra, "Enhancement of Breakdown Voltage in AlGaIn/GaN High Electron Mobility Transistors Using a Field Plate", IEEE Trans. Electron Devices, vol. 48, pp. 1515-1521, 2001.
4. W.-C. Cheng, T. Fang, S. Lei, Y. Zhao, M. He, M. Chan, G. Xia, F. Zhao, and H. Yu, "Silicon Nitride Stress Liner Impacts on the Electrical Characteristics of AlGaIn/GaN HEMTs," Proc. EDTM, 2019.
5. Y. Ando, Y. Okamoto, H. Miyamoto, T. Nakayama, T. Inoue, and M. Kuzuhara, "10-W/mm AlGaIn-GaN HFET with a field modulating plate," IEEE Electron Device Lett., vol. 24, pp. 289–291, 2003.
6. R. J. Trew, U. K. Mishra, "Gate breakdown in MESFETs and HEMTs", IEEE Electron Device Letters, vol. 12, 524-527, 1991.
7. H. Chiu, C. Yang, H. Wang, F. Huang, H. Kao, and F. Chien, "Characteristics of AlGaIn/GaN HEMTs With Various Field-Plate and Gate-to-Drain Extensions," in IEEE Transactions on Electron Devices, vol. 60, pp. 3877-3882, 2013.
8. H. Xing, Y. Dora, A. Chini, S. Heikman, S. Keller, and U. K. Mishra, "High breakdown voltage AlGaIn-GaN HEMTs achieved by multiple field plates," IEEE Electron Device Letters, vol. 25, pp. 161-163, 2004.
9. S. Joglekar, C. Lian, R. Baskaran, Y. Zhang, T. Palacios, and A. Hanson, "Finite Element Analysis of Fabrication- and Operation-Induced Mechanical Stress in AlGaIn/GaN Transistors," IEEE Transactions on Semiconductor Manufacturing, vol. 29, pp. 349-354, 2016.
10. VictoryDevice User's manual, 2017.
11. VictoryStress User's manual, 2017.

## AUTHORS PROFILE



**Mr. Rajib Kumar Nanda** has received his B.Tech Degree in Electronics and Telecommunication Engineering from University College of Engineering, Burla, India in 2008, and M.Tech Degree in Electronics and Communication Engineering from IIT Kharagpur, India in 2015. He is currently working as an Assistant Professor at Siksha 'O' Anusandhan (Deemed to be) University, Bhubaneswar, India, and is also pursuing his Ph.D. Degree in Electronics and Communication Engineering. His research interest lies in Device modeling and simulation.



**Mr. Tara Prasanna Dash** has received his degree of Bachelor of Technology in Electronics and Telecommunication Engineering from Biju Patnaik University of Technology, India in 2009 and master degree in Electronics Communication Engineering from Indian Institute of Technology Kharagpur, Kharagpur, India in 2012. He is currently working as an Assistant Professor at Siksha 'O' Anusandhan (Deemed to be University) and is pursuing his PhD in heterojunction devices. His research interests include performance analysis of 2D and 3D devices using TCAD tools.